Wind field retrieval from SAR compared with scatterometer wind field during ERS Tandem phase

E. Korsbakken & B. Furevik

Nansen Environmental and Remote Sensing Centre
Edv. Griegsvei 3a, N-5037 Solheimsviken, Bergen, Norway
Phone: 47-55.29 72 88, Fax: 47-55.20 00 50, E-mail: Erik.Korsbakken@nrsc.no

An evaluation of wind retrieval by SAR has been performed by comparing computed winds from ERS-2 SAR with ERS-1 microwave scatterometer measurements. This was possible during the Tandem phase of the ERS project, for latitudes greater than about 63°. In this case the scatterometer and SAR coverage overlapped with a time difference of only 30 minutes. Preliminary results confirm the usefulness of SAR in determining wind speed at high spatial resolution, provided that some information on wind direction can be obtained (e.g. from wind streaks).

Although the comparison was performed over the Norwegian/Greenland Sea, the results will be applicable to retrieving wind over lower-latitude areas and in coastal regions, at a resolution better than the 50 km resolution obtainable from the scatterometer.

Introduction

Several recent works [such as *Vachon et al.* 1996, *Scoon et al.* 1996 and *Korsbakken et al.* 1997] report promising results when wind retrieval models developed for the wind scatterometer (WSC) are applied to SAR data. The general conclusion from these works is that more validation is needed since the available in-situ material is relatively limited. A dataset from the ERS-1/2 Tandem phase allows for a new type of validation study of the wind retrieval models when applied to SAR, and validate the results towards the scatterometer derived wind field with 30 minutes lag. The orbit configuration and the wide swath of the WSC cause an overlap at latitudes greater than about 63°.

In this work we discuss the major difference of two C-band models and their performance and the novel comparison of SAR and WSC wind field. In the first section we give a brief overview of the data used followed by a discussion of stationary in the wind field before the results are presented and, finally, a summary is given.

Data analysis

As seen from Table 1 there is a total of 36 ERS-2 SAR images from 6 different days is available together with the corresponding scatterometer wind field from the ERS-1. This provides more than 150 collocated WSC wind vectors within the SAR images for validation where the wind speed ranges from about 3 to 17 m/s. At 50 km WSC resolution (the nominal resolution provided by ESA), the wind vectors are computed from overlapping 50 km wide cells (spatial resolution) every 25 km (grid spacing). The WSC wind vectors is therefore not fully independent.

Included in the study are also pressure maps from the hindcast database (produced by the Norwegian Meteorological Institute) at 06:00 and 12:00 UTC to indicate the current weather situations. Figure 1 shows two examples of maps of the area west of Greenland with the WSC wind data and 12:00 UTC isobars. The overlaid boxes indicate the geographical location of the corresponding analysed SAR scenes.

The scatterometer wind field from 1 September (Fig.1, top, reveals a strong wind front connected with a low-pressure centre. 12 SAR images are available from the vicinity of the low pressure and passes through the front associated with strong winds (16-17 m/s) to the south. The surface signatures in the SAR image south of the front are dominated by wind streaks. In the south the wind drop to less than 5 m/s and the backscatter in the SAR images has a great variability due to eddies, surface slicks and internal waves that becomes visible in the weak

Table 1. Data used in the study.

ERS-1 WSC		ERS-2 SAR	
Date	*Orbit*	*Orbit*	*Frame*
950822	21454	01767	2133, 2151, 2169, 2187, 2205, 2223, 2241, 2259
950825	21497	01810	2223, 2241
950901	21597	01910	2025, 2043, 2061, 2079, 2097, 2115, 2133, 2151, 2169, 2187, 2205, 2223
950911	21740	02053	2133, 2151, 2169, 2187, 2205, 2223
950917	21826	02139	2205, 2223, 2241
950927	21969	02282	2187, 2205, 2223, 2241, 2259

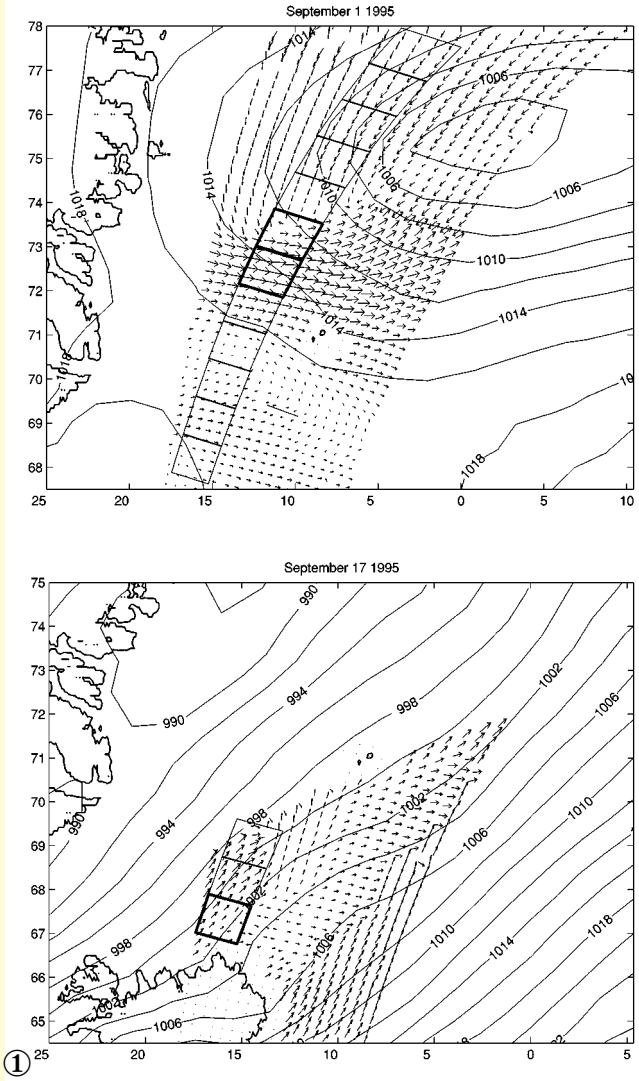

Wind field in the Greenland Sea from 1 September (top) and 17 September (bottom) 1995 as measured by the ERS-1 scatterometer. The length of the arrows indicate the relative wind speed and the they are oriented in the direction the wind is blowing. The overlaid boxes are the positions of the ERS-2 SAR images. The ERS-2 passes the area approximately half an hour after the ERS-1. Overlaid are the isobars from the hindcast database.

wind. The image covering the front is shown in Figure 2.

In the situation from 17 September (Fig.1, bottom), Iceland is clearly acting as an obstacle to the wind field and the effect is seen as some sort of spiralling wind field, judged from the changes in wind direction. The effect is seen to the northeast of Iceland as far as the WSC data is covering, which is some 1000 km from the shore. The wind speed measured from the scatterometer reaches 14.6 m/s in the northeast.

In the data comparisons we assume the sea surface to be stationary during the 30 minute time lag between the WSC and the SAR image data. This assumption is justified by identification of similar features in the WSC and SAR image data. In the first case (1 September) we observe a strong wind front in the WSC wind field crossing through a SAR image as noted before. This image is shown in Figure 2 and here we clearly see the change in backscatter associated with a wind front. The second example is from 17 September where we observe the lee effect from Iceland in the WSC wind field as discussed above. In the last of the three SAR images from that day, we would expect backscatter signatures of low winds to the east and stronger winds to the west. This is also confirmed by the dark patches to the right in the image (Fig. 3), and the higher backscatter with some atmospheric wind dependent features to the left. The geographical positions of the observed fronts in the SAR and WSC data are in correspondence with each other.

C-band models

The radar scatterometer measure the radar NRCS quantitatively and an amplitude-calibrated radar can be a scatterometer. Interpretation of observations with scatterometers led to the conclusion that the NRCS is proportional to some power of the wind speed. This relation has then been improved during several experiments to include NRCS dependence of wind speed, wind direction and incidence angle. The CMOD4 model [*Stoffelen & Anderson* 1994] has been used at the European Centre for Medium-Range Weather Forecasting (ECMWF) during the lifetime of the ERS-1 and followed by the ERS-2 scatterometer. The CMOD4 model is empirically tuned to the ECMWF weather model results. The similar CMOD Ifremer [*Quilfen et al.* 1997] is calibrated against in-situ measurements, in particular NOAA buoys and partly ECMWF model results in order to provide measurements compatible with other wind measurement systems such as buoys, altimeters and radiometers. For practical use series of theoretical NRCS are computed as a function of incidence angle and wind direction. In turn, the theoretical NRCS are used as a look-up table to compare with NRCS measured in the SAR image.

Figure 4 shows profiles of both the CMOD4 and the CMOD Ifremer

SAR image from 1 September 1995 showing a strong wind front.

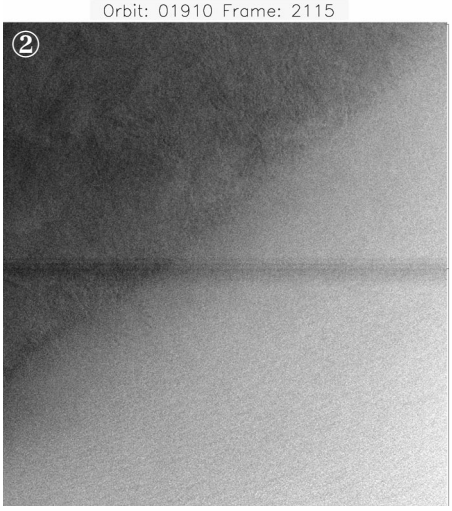

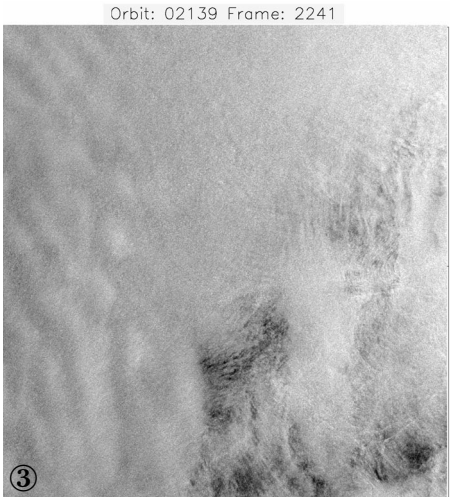

SAR image from 17 September 1995 showing decreased intensity due to lee effects in the region north east of Iceland.

algorithms. We observe that the CMOD4 gives lower NRCS in the low wind part (from 2 to 4 m/s) compared to the CMOD Ifremer and higher NRCS in the wind speed range from about 4 to 18 m/s. Used as a look-up table the CMOD4 will give lower wind speeds than the CMOD Ifremer in the 4 to 18 m/s region and vice versa outside this region. Concerning the high wind part of the C-band models, corresponding in-situ observations and SAR data under high wind speed conditions are uncommon. Meteorological model results under such conditions also suffer from uncertainties in the in-situ measurements. In turn, this limits the available C-band model validation data and the model must be considered as an extrapolation of the shape for moderate to high winds [*Quilfen et al.* 1997].

A major limitation of using C-band models in SAR images is the demand for external knowledge of the wind direction. As discussed in *Johannessen et al.* [1995] the wind direction may be derived directly from the low-frequency part of the SAR image power spectrum showing the orientation of the wind streaks or meteorological maps. In this analysis we use the wind direction from the WSC which allows for a direct comparison of wind speeds.

Optimal wind speed estimate from a C-band model will depend on the radiometric capabilities of the SAR to reproduce the NRCS. Several calibrations of the raw SAR data are necessary and a reprocessing of the SAR data according to *Laur et al.* [1997] is performed. In particular, the analog-to-digital conversion power loss, due to saturation in the binary representation of the signal in the satellite, is corrected. (A further discussion of the absolute calibration is beyond the scope of this work.)

In Figures 5 and 6 the scatterplots of comparing WSC and SAR-derived wind speed using the CMOD4 and the CMOD Ifremer is shown. The SAR spatial resolution is 25 x 25 km and wind speed estimates from all 36 SAR images are included. The classification codes from manual classification of the sub-images as explained later, is only used when the wind speed difference is more than 2 m/s to identify those areas. Moreover, for the CMOD4 algorithm, shown in Figure 5, there seem to be three regimes; for low wind speeds (< 5 m/s) the correlation is good; at medium to high wind speeds the majority of the wind speeds are underestimated compared to the WSC and the SAR wind speed is also slightly underestimated for high wind speeds (> 15 m/s). Regarding the points of more than ±2 m/s wind speed difference we see from the plot that c3 (homogenous sub-images) dominates among c1 (wind front), c2 (periodic signatures) and c3 points. This result was in contrast to what we expected for any eventual fliers which we believed to be dominated by inhomogeneous sub-images.

The wind algorithm used to process the WSC off-line product is the CMOD Ifremer. As expected we see a better agreement when using this model to derive wind speeds from the SAR data. The scatter plot in Figure 6 seems to split in two, with obvious underestimation for winds lower than about 5 m/s and slight underestimation for the majority of the points above 5 m/s. Here we also find some homogenous sub-images (c3) of wind speed more than 2 m/s compared to the WSC wind speed.

Discussion and conclusion

Comparison of WSC and C-band model SAR derived wind speeds for more than 150 measurements and for a large variability of wind speeds and directions have been performed. The results support the practice of applying existing C band models to SAR with better spatial resolution to get the wind speed if external knowledge of wind direction can be provided. An overall assessment of the CMOD4 and the CMOD Ifremer shows no significant difference in the error estimates when the model results are compared to WSC wind speed. There are some differences related to different ranges of wind speeds and we have seen that the CMOD4 compares better below 4 m/s, whereas the CMOD Ifremer shows better performance above 4 m/s. If the observed biases in the CMOD4 and CMOD Ifremer comparison to the WSC

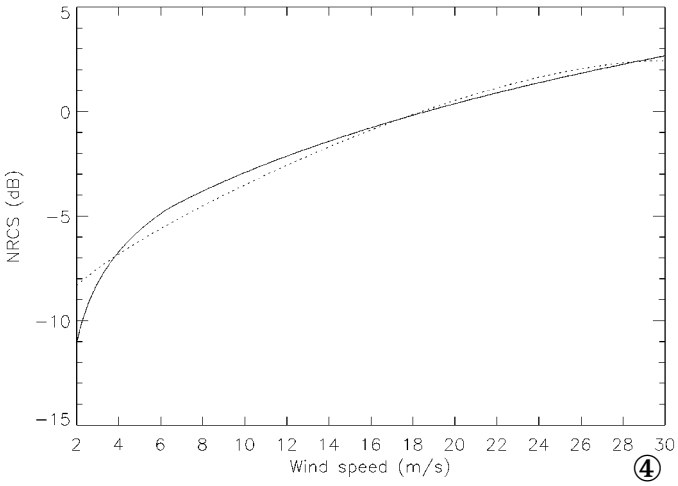

Comparison of CMOD4 (solid line) and CMOD Ifremer (dashed line).

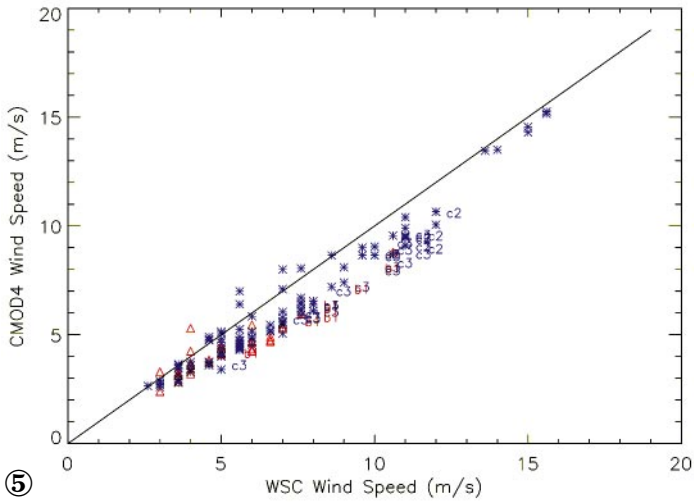

⑤ *CMOD4 wind speed vs. SWA wind speed.*

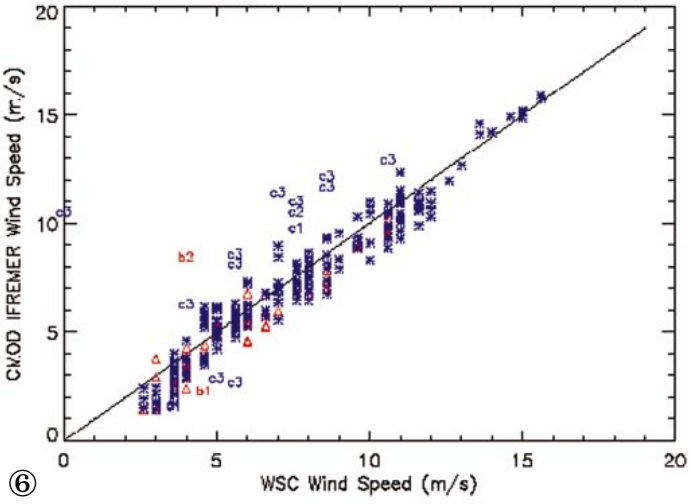

⑥ *CMOD Ifremer vs. SWA wind speed.*

wind speed were related to rapid changes in the surface wind field during the 30 minute time-lag we would have expected a more widely scattered plot based on the relative large variety in wind speed and wind direction for the six different days.

In the study of *Korsbakken et al.* [1997] an underestimation was observed when comparing the CMOD4 results to in-situ measurements, this suggest that the CMOD Ifremer will perform better providing higher wind speeds in the actual range.

From the analysis we also see that both the CMOD4 and the CMOD Ifremer catches the limited number of higher wind speeds in the dataset but still the SAR response of wind speed higher than 15 m/s has been little investigated and the performance of applying C-band models developed for scatterometer is unpredictable.

We have also noticed that there is no obvious dependence on the spatial resolution of the behaviour of the WSC SAR wind speed comparison. In the analyses we tested spatial resolutions of 4x4, 10x10 and 25x25 km in SAR image without notice any significant variations. This indicates that the scatterometer algorithms still works for spatial resolutions higher than the wind scatterometer. This is also consistent with previous studies of the variability in the NRCS du to the spatial resolution, see e.g. Korsbakken et al. [1997]. Since the CMOD Ifremer validated against temporary averaged in-situ measurements another important conclusion is that the wind derived from the SAR corresponds to the same temporal averaged wind.

Acknowledgements
Data for this study was provided by ESA at AOT.N302. E. Korsbakken & B. Furevik were supported by a strategic SAR program at the Nansen Centre in conjunction with the Norwegian Research Council.

References

Johannessen JA, PW Vachon & OM Johannessen, ERS-1 SAR imaging of marine boundary layer processes, *Earth Observation Quarterly*, ESA, 1995.

Johannessen OM et al., Coast Watch '95 ERS-1,2 SAR applications of mesoscale upper ocean and atmospheric boundary layer processes off the coast of Norway, *IGARSS '96*, Lincoln, Nebr., 1996.

Korsbakken E, JA Johannessen & OM Johannessen, Coastal wind field retrievals from ERS synthetic aperture radar images, accepted in *JGR*, 8 Sept. 1997.

Laur H, P Bally, P Meadows, PJ Sanchez, B Schaettler & E Lopinto, Derivation of the backscattering coefficient s0 in ESA ERS SAR PRI products, Doc. *ES-TN-RS-PM-HL09*, issue 2, rev. 2, ESRIN, Frascati, Italy, 28 June 1996.

ScoonA, TS Robinson & PJ Meadows, Demonstration of an improved calibration scheme for ERS-1 SAR imagery using a scatterometer wind model, *Int. J. Remote Sens*. **17** (2), 413-418, 1996.

Stoffelen A & DLT Anderson, ERS-1 scatterometer data and Characteristics and wind retrieval skills, *Proc. First ERS-1 Symp., ESA SP-359*, 1993.

Vachon PW & FW Dobson, Validation of wind vector retrieval from ERS-1 SAR images over the ocean, *The Global Atm. & Ocean Sys.* **5**, 177-187, 1996.

Quilfen Y, B Chapron, T Elfouhaily, K Katsaros & J Tournadre, Observation of tropical cyclones by high-resolution scatterometry, accepted in *JGR*, 3 July 1997.